Hierarchical Multilevel Potential Preconditioner for Fast Finite-Element Analysis of Microwave Devices

Yu Zhu, *Student Member, IEEE,* and Andreas C. Cangellaris, *Fellow, IEEE*

***Abstract*—A robust hierarchical multilevel preconditioning technique is presented for the fast finite-element analysis of microwave devices. The proposed preconditioner is based on a hierarchical multilevel scheme for the vector–scalar potential finite-element formulation of electromagnetic problems. Numerical experiments from the application of the new preconditioner to the finite-element analysis of microwave devices are used to demonstrate its superior numerical convergence and efficient memory usage.**

***Index Terms*—Finite-element method, hierarchical basis functions, hierarchical multilevel, vector and scalar potential formulation.**

I. Introduction

THE finite-element method (FEM) is one of the most effective and versatile techniques for the modeling of complex microwave devices [1]. Its application to practical engineering problems often results in large linear systems requiring iterative methods for their numerical solution. However, the convergence of iterative solvers tends to be unpredictable for electromagnetic-wave problems, even when common preconditioners, such as incomplete LU factorization, are used to improve convergence.

The reasons for the slow convergence of the iterative solver are by now well understood. They are associated with the dc modes contained in the null space of the curl operator, and the ill conditioning of the FEM matrix resulting from the oversampling of the low-frequency physical modes [2]. As was proposed in [3], the spurious dc modes can be canceled by introducing a spurious electric charge and imposing the divergence-free condition $\nabla \cdot \vec{D} = 0$, explicitly in the weak statement of the electromagnetic problem. Use of the vector–scalar potential ($\vec{A} - V$) formulation for the development of the FEM approximation is most suitable for this purpose. On the other hand, the difficulties associated with low-frequency physical modes can be tackled effectively by solving problems tentatively on coarser grids [4] or in lower order basis function spaces. More specifically, those modes that are oversampled on the original FEM grid can be solved without loss of accuracy using an FEM system with much fewer degrees of freedom. Subsequently, through an interpolation process, the generated numerical solutions are projected back onto the original grid on which the higher frequency modes are to be calculated accurately.

The demonstrated success of these remedies prompted their combination into a multigrid vector–scalar potential finite-element preconditioner that was shown to exhibit outstanding convergence in conjunction with the analysis of two- and three-dimensional electromagnetic problems [5], [6]. There are two types of multigrid techniques, i.e., geometric and hierarchical. The geometric multigrid technique uses a set of nested multigrids obtained by dividing each tetrahedron in the coarsest grid into eight equal-volume sub-tetrahedra; hence, the geometric multigrid technique functions as an h-adaptive FEM. Its application to electromagnetic problems has been presented in [4]–[6]. However, for those cases where the domain under study contains sub-domains where the electromagnetic field variation is sufficiently smooth, it is found that p-adaptive schemes can tackle numerical dispersion error more effectively than h-adaptive ones. Therefore, in this paper, a hierarchical multilevel vector–scalar potential finite-element preconditioner is proposed that uses only one grid and a set of hierarchical basis function spaces, i.e., $H^0(\mathrm{curl})$ and $H^1(\mathrm{curl})$, for the FEM approximation and solution of the electromagnetic boundary-value problem.

The use of a hierarchical preconditioner and a so-called $\vec{E}$-field Schwartz solver for the FEM solution of the electromagnetic boundary-value problem was proposed in [7] and [8]. Although the proposed solver showed much faster convergence compared to other commonly used FEM solvers, its implementation of the divergence-free condition is not complete, in the sense that the lowest order scalar basis functions are missing. The technique proposed in this paper can be understood as an $\vec{A} - V$ potential Schwartz solver that overcomes this deficiency and yields a hierarchical multilevel FEM solver with superior convergence and numerical robustness.

The paper is organized as follows. First, the FEM approximations for the $\vec{E}$-field and $\vec{A} - V$ potential formulations of the electromagnetic problem are developed on the $H^0(\mathrm{curl})$ and $H^1(\mathrm{curl})$ spaces. Through this development, those attributes of the potential formulation that improve the convergence of the iterative matrix solution process are highlighted. Next, the hierarchical multilevel potential preconditioner is presented. This paper concludes with the application of the proposed preconditioner to the electromagnetic analysis of rectangular waveguide and microstrip devices. These numerical studies help validate the computer implementation of the new method and demonstrate its superior convergence properties.

Manuscript received August 17, 2001. This work was supported in part by the Semiconductor Research Corporation under a Texas Instruments Incorporated Custom Research Grant, and in part by the Motorola Center for Communications, College of Engineering, University of Illinois at Urbana-Champaign.

The authors are with the Department of Electrical and Computer Engineering, University of Illinois at Urbana-Champaign, Urbana, IL 61801 USA (e-mail: cangella@uiuc.edu).

Publisher Item Identifier 10.1109/TMTT.2002.801351.

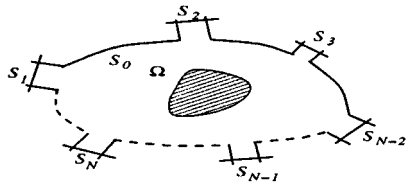

Fig. 1. Multiport electromagnetic device.

II. Field Formulation

Consider a three-dimensional multiport electromagnetic device with the generic schematic representation depicted in Fig. 1. For the purposes of this paper, all media are assumed to be linear, isotropic, nonmagnetic, and time invariant. The weak statement of the governing electric-field vector Helmholtz equation

$$\nabla \times \nabla \times \vec{E} - \omega^2 \mu_0 \epsilon_0 \epsilon_r \vec{E} = 0 \tag{1}$$

is well known and is given by

$$\int_\Omega \nabla \times \vec{w} \cdot \nabla \times \vec{E}\, dv - j\omega\mu_0 \oint_{\partial\Omega} \hat{n} \times \vec{H} \cdot \vec{w}\, ds - \omega^2 \mu_0 \epsilon_0 \int_\Omega \vec{w} \cdot \epsilon_r \vec{E}\, dv = 0 \tag{2}$$

where $\vec{w}$ is the FEM basis function used for the numerical approximation of the vector electric field. In order to address the general case, the computational domain Ω is assumed to be bounded by both microwave port boundaries S_i, $i = 1, 2, \ldots, N$, and a numerical truncation boundary S_0 on which a first-order absorbing boundary condition is imposed to model the associated unbounded region.

Without loss of generality, it is assumed that each microwave port is associated with the cross section of a waveguide with known modal solutions. This is typically the case for most practical multiport microwave devices of interest. Furthermore, to simplify the mathematical statement of the weak formulation of the electromagnetic problem, and without loss of generality, it is assumed that, at each waveguide port, only the fundamental mode propagates. Following standard microwave circuit analysis procedures, let S_1 be the excitation port. The weak form of the driven problem becomes

$$\int_\Omega \nabla \times \vec{w} \cdot \nabla \times \vec{E}\, dv + jk_0 \int_{S_0} \hat{n} \times \vec{w} \cdot \hat{n} \times \vec{E}\, ds + \sum_{i=1}^{N} jk_{z,i} \int_{S_i} \hat{n} \times \vec{w} \cdot \hat{n} \times \vec{E}\, ds - \omega^2 \mu_0 \epsilon_0 \int_\Omega \vec{w} \cdot \epsilon_r \vec{E}\, dv = 2jk_{z,1} \int_{S_1} \hat{n} \times \vec{w} \cdot \hat{n} \times \vec{e}_1\, ds \tag{3}$$

where $k_{z,i}$ is the propagation constant for the single propagating mode at the ith port, and $\vec{e}_i$ is the associated normalized electric-field distribution of the mode on S_i. Once the numerical solution has been obtained, the reflection coefficient at port S_1 and the transmission coefficients at the remaining ports are obtained as follows:

$$S_{11} = \int_{S_1} \hat{n} \times \vec{E} \cdot \vec{h}_1\, ds - 1$$
$$S_{i1} = \int_{S_i} \hat{n} \times \vec{E} \cdot \vec{h}_i\, ds \tag{4}$$

where $\vec{h}_i$ is the associated normalized magnetic-field distribution of the mode on S_i.

Following Galerkin's approach, the testing functions $\vec{w}$ and the expansion functions for $\vec{E}$ are the bases in the tangentially continuous vector (TV) spaces [9]. The ith TV space is $H^i(\mathrm{curl})$, for which both its basis functions and their $curl$ are complete to the ith order vector polynomial functions [8], [9].

The lowest (zeroth-order) order TV space is $H^0(\mathrm{curl})$, often referred to as "edge elements." For each edge(i, j), there is one basis function in $H^0(\mathrm{curl})$ space as follows:

$$H^0(\mathrm{curl}) = \mathrm{span}\{\zeta_i \nabla\zeta_j - \zeta_j \nabla\zeta_i\}. \tag{5}$$

The first-order TV space can be written as

$$H^1(\mathrm{curl}) = H^0(\mathrm{curl}) \oplus \nabla W^2_{s,e} \oplus R^2_{\mathrm{tv},f} \tag{6}$$

where $W^2_{s,e}$ represents the second-order edge-type scalar subspaces [9], the gradient of which is added to make bases in $H^1(\mathrm{curl})$ complete to first-order polynomials. For each edge (i, j), there is one basis function in $W^2_{s,e}$

$$W^2_{s,e} = \mathrm{span}\{\zeta_i \zeta_j\}. \tag{7}$$

Finally, $R^2_{\mathrm{tv},f}$ denotes the second-order face-type nongradient TV subspace [9], the addition of which makes the curl of the bases in $H^1(\mathrm{curl})$ complete to first-order polynomials. For each face (i, j, k), there are two basis functions in $R^2_{\mathrm{tv},f}$ as [8]

$$R^2_{\mathrm{tv},f} = \mathrm{span}\Big\{4\zeta_i\big(\zeta_j\nabla\zeta_k - \zeta_k\nabla\zeta_j\big),\ 4\zeta_j\big(\zeta_k\nabla\zeta_i - \zeta_i\nabla\zeta_k\big)\Big\}. \tag{8}$$

Use of $H^1(\mathrm{curl})$ yields the following FEM matrix for the weak statement (3):

$$\begin{pmatrix} M^{11}_{EE} & M^{10}_{EE} \\ M^{01}_{EE} & M^{00}_{EE} \end{pmatrix} \begin{pmatrix} x^1_E \\ x^0_E \end{pmatrix} = \begin{pmatrix} f^1_E \\ f^0_E \end{pmatrix} \tag{9}$$

where x^0_E contains the expansion coefficients for $H^0(\mathrm{curl})$, and x^1_E contains the expansion coefficients for $\nabla W^2_{s,e} \oplus R^2_{\mathrm{tv},f}$. The specific forms of the entries of M^{ij}_{EE} are easily deduced through a direct comparison with (3).

As it has been elaborated in [2] and [5], the direct application of an iterative solver, such as conjugate gradient (CG), to the solution of the FEM matrix exhibits slow convergence. The reason is that, at the specific operating frequency, all dc modes and some low-frequency ones below the operating frequency are shifted to the left-hand side of the frequency plane, thus rendering the system matrix highly ill conditioned. Common preconditioners, such as incomplete Cholesky factorization, tend to perform very poorly [2]. The additive or multiplicative Schwartz preconditioner of (9), which uses direct factorization at the $H^0(\mathrm{curl})$ level, has been shown to exhibit faster convergence [7]. In this paper, we propose to apply the Schwartz technique to the vector and scalar potential formulation.

III. Potential Formulation

As already mentioned in Section I, the spurious dc modes can be suppressed by using the vector and scalar potential formulation to impose the divergence-free condition on the electric field explicitly. In addition, the low-frequency modes can be pre-solved accurately in the $H^0(\mathrm{curl})$ space. These observations

motivate the proposition for a hierarchical multilevel potential preconditioner to tackle the convergence difficulties associated with the iterative solution of the electromagnetic FEM system. The development of the proposed preconditioner begins with the discussion of the hierarchical potential formulation. This is followed by the presentation of the algorithm for the multilevel preconditioner, given in the following section.

Following [3] and [5], the electric field is written as $\vec{E} = \vec{A} + \nabla V$. Thus, the weak form of the curl–curl equation for the electric field (1) becomes

$$\begin{aligned}\int_\Omega \nabla\times\vec{w}\cdot\nabla\times\vec{A}\,dv + jk_0\int_{S_0}\hat{n}\times\vec{w}\cdot\hat{n}\times\left(\vec{A}+\nabla V\right)ds \\ +\sum_i jk_{z,i}\int_{S_i}\hat{n}\times\vec{w}\cdot\hat{n}\times\left(\vec{A}+\nabla V\right)ds \\ -\omega^2\mu_0\epsilon_0\int_\Omega \vec{w}\epsilon_r\left(\vec{A}+\nabla V\right)dv \\ = 2jk_{z,1}\int_{S_1}\hat{n}\times\vec{w}\cdot\hat{n}\times\vec{e}_1\,ds. \end{aligned} \tag{10}$$

The weak form of the divergence-free equation $\nabla\cdot\vec{D} = 0$ is obtained through its multiplication with the gradient of the scalar basis function $\nabla\phi$ and the subsequent integration over the volume of interest. This yields

$$\begin{aligned} jk_0\int_{S_0}\hat{n}\times\nabla\phi\cdot\hat{n}\times\left(\vec{A}+\nabla V\right)ds + \sum_i jk_{z,i}\int_{S_i}\hat{n}\times\nabla\phi \\ \cdot\hat{n}\times\left(\vec{A}+\nabla V\right)ds - \omega^2\mu_0\epsilon_0\cdot\int_\Omega\nabla\phi\cdot\epsilon_r\left(\vec{A}+\nabla V\right)dv \\ = 2jk_{z,1}\int_{S_1}\hat{n}\times\nabla\phi\cdot\hat{n}\times\vec{e}_1\,ds. \end{aligned} \tag{11}$$

For the $H^0(\mathrm{curl})$ potential formulation, the functions $\vec{w}$ and ϕ are chosen as

$$\vec{w}\in H^0(\mathrm{curl}), \qquad \phi\in W^1_{s,n}, \tag{12}$$

where $W^1_{s,n}$ is the first-order node-type scalar subspace [9]

$$W^1_{s,n} = \{\zeta_0, \zeta_1, \zeta_2, \zeta_3\}. \tag{13}$$

For an $H^1(\mathrm{curl})$ potential formulation, the following choice must be made:

$$\vec{w}\in H^0(\mathrm{curl})\oplus R^2_{\mathrm{tv},f} \quad \phi\in W^1_{s,n}\oplus W^2_{s,e}. \tag{14}$$

That is, the basis functions in $H^1(\mathrm{curl})$ are decomposed into two parts. The part containing the nongradient subspaces $H^0(\mathrm{curl})$ and $R^2_{\mathrm{tv},f}$ is used to expand the vector potential, while the part containing the gradient subspaces $W^1_{s,n}$ and $W^2_{s,e}$ is used to expand the scalar potential. Finally, as it has been elaborated in [3] and [9], $\nabla W^1_{s,n}$ is a subset of $H^0(\mathrm{curl})$. Thus, a transition matrix G exists between the two spaces such that

$$\nabla W^1_{s,n} = H^0(\mathrm{curl})G. \tag{15}$$

In view of the above, the matrix representation of (10) and (11) may be cast in a hierarchical form as follows:

$$\begin{pmatrix} M^{11}_{AV} & M^{10}_{AV} \\ M^{01}_{AV} & M^{00}_{AV}\end{pmatrix}\begin{pmatrix} x^1_{AV} \\ x^0_{AV}\end{pmatrix} = \begin{pmatrix} f^1_{AV} \\ f^0_{AV}\end{pmatrix} \tag{16}$$

where the vector x^0_{AV} contains the expansion coefficients for $H^0(\mathrm{curl})\oplus\nabla W^1_{s,n}$, while the vector x^1_{AV} contains the ones for $R^2_{\mathrm{tv},f}\oplus\nabla W^2_{s,e}$. The entries of the matrices M^{ij}_{AV} are evident through a direct comparison of (10) and (11) with (16).

Alternatively, the more traditional matrix form of (10) and (11) that separates the vector and scalar potentials is

$$\begin{pmatrix} P_{AA} & P_{AV} \\ P_{VA} & P_{VV}\end{pmatrix}\begin{pmatrix} x_A \\ x_V\end{pmatrix} = \begin{pmatrix} f_A \\ f_V\end{pmatrix} \tag{17}$$

where x_A contains the expansion coefficients for $\vec{A}$, while x_V contains the ones for V. In this form, it is clearly seen that the divergence-free condition is imposed explicitly.

IV. Transformation Between the Two Formulations

The hierarchical field and potential formulations are equivalent. Their equivalency can be proven through careful examination of (9) and (16). Due to the bilinear form of the system matrices and the linear form of the right-hand sides, it is

$$\begin{aligned} f^1_{AV} &= f^1_E \\ f^0_{AV} &= \begin{pmatrix} I \\ G^T\end{pmatrix} f^0_E \end{aligned} \tag{18}$$

and

$$\begin{aligned} M^{11}_{AV} &= M^{11}_{EE} \\ M^{10}_{AV} &= M^{10}_{EE}(I, G) \\ M^{01}_{AV} &= \begin{pmatrix} I \\ G^T\end{pmatrix} M^{01}_{EE} \\ M^{00}_{AV} &= \begin{pmatrix} I \\ G^T\end{pmatrix} M^{00}_{EE}(I, G) \end{aligned} \tag{19}$$

and

$$\begin{aligned} x^1_E &= x^1_{AV} \\ x^0_E &= (I, G)x^0_{AV}. \end{aligned} \tag{20}$$

In the above, I denotes the identity matrix. Using (18), the right-hand sides in the field formulation can be transformed to the ones in the potential formulation. Using (20), the solutions in potential formulation can be transformed back to the ones of field formulation. Hence, the transformation between the two formulations is straightforward and enables the following methodology for the construction of a robust preconditioner for a spurious mode-free iterative solution of (9).

V. Hierarchical Multilevel Potential Preconditioner

Consider the calculation of the pseudoresidual equation in each step of the iterative solution of (9) as follows:

$$\begin{pmatrix} M^{11}_{EE} & M^{10}_{EE} \\ M^{01}_{EE} & M^{00}_{EE}\end{pmatrix}\begin{pmatrix} z^1_E \\ z^0_E\end{pmatrix} = \begin{pmatrix} r^1_E \\ r^0_E\end{pmatrix}. \tag{21}$$

The following smoothing technique can be used as a single-level preconditioner. First, (21) is transformed to the matrix equation of the potential formulation using (18) and (19). Next, in the

potential formulation, the matrix equation (17) is solved in two steps. Step 1 involves the solution of z_A from the following:

$$P_{AA}z_A = r_A - P_{AV}z_V. \tag{22}$$

Step 2 explicitly imposes the divergence-free condition in order to suppress the spurious dc modes to a certain level by solving z_V through the following:

$$P_{VV}z_V = r_V - P_{VA}z_A. \tag{23}$$

Both of the above are approximate solutions and are effected either through an incomplete Cholesky factorization or through the Gauss–Seidel method. Finally, once the solution for the potential formulation is obtained, it is transformed back to the field formulation using (20).

However, as already mentioned previously, the single-level potential preconditioner cannot tackle efficiently the ill conditioning caused by low-frequency modes. To overcome this difficulty and improve convergence, the above (single-level) preconditioning process is combined with multilevel techniques. This extension of the single-level preconditioner to a multilevel one is described in the following typical multilevel pseudocode MG(r_E, z_E, i).

1) $z_E \leftarrow 0$,
2) if $i == 0$, then solve $M_{EE}z_E = r_E$. // lowest level
3) else
   3a) smooth(z_E, r_E) for v_1 times.
   3b) $r_E^{i-1} \leftarrow I_i^{i-1}(r_E - M_{EE}z_E)$
   3c) MG(z_E^{i-1}, r_E^{i-1}, $i-1$)
   3d) $z_E \leftarrow z_E + I_{i-1}^{i} z_E^{i-1}$
   3e) smooth(z_E, r_E) for v_2 times.

Smooth(z_E, r_E) denotes in a short-hand notation the single-level potential preconditioner discussed at the beginning of this section. I_i^{i-1} is the restriction operator that maps the residual of the ith level matrix equation down to the $(i-1)$th level. I_{i-1}^{i} is the interpolation operator that interpolates the correction obtained on the $(i-1)$th level back to the ith level. The use of the hierarchical basis functions facilitates greatly the implementation of these operations.

The proposed preconditioner constitutes an $\vec{A} - V$ potential multiplicative Schwartz preconditoner instead of the $\vec{E}$-field Schwartz preconditioner proposed in [7]. It uses direct factorization on the lowest level block of $H^0(\mathrm{curl})$, and Gauss–Seidel on the higher level block. The Schwartz operation is applied to the matrix equation of the potential formulation so that the imposition of the divergence-free constraint is implemented in the second-order complete scalar space $W_{s,n}^1 \oplus W_{s,e}^2$.

VI. Numerical Results

The proposed preconditioners can be combined with a Krylov subspace-based iterative solver, such as CG or generalized minimum residual method (GMRES). In the following tests, CG was used. The stopping criterion used for the iterative solver was

$$\frac{\|r\|_\infty}{\|f\|_\infty} = \mathrm{tol}, \qquad \mathrm{tol} = 1.0e{-}6 \tag{24}$$

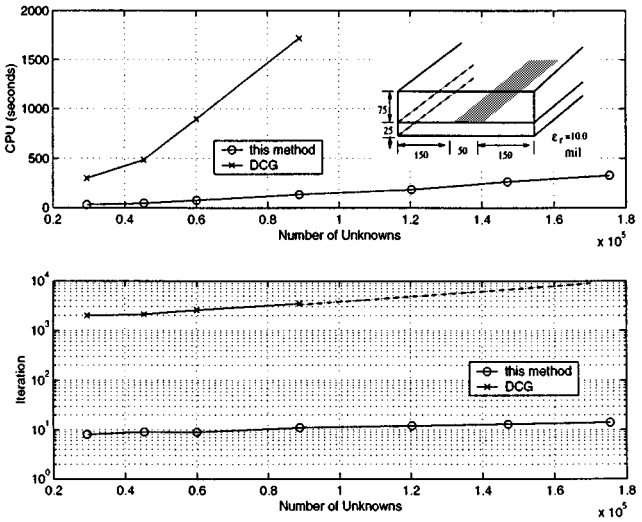

Fig. 2. CPU time and number of iterations versus the number of unknowns for a microstrip line.

where f is the right-hand-side vector of the matrix equation assuming the initial guess vector is zero. In all cases, the number of pre-smoothing and post-smoothing operations was taken to be $v1 = v2 = 3$. All calculations were performed on a Pentium III 600-MHz PC.

Fig. 2 shows the CPU time and number of iterations required for convergence versus the number of unknowns for the simple geometry of a microstrip line. The operating frequency is 20 GHz. The number of unknowns is varied by adjusting the line length from 200 to 1200 mil (i.e., $\sim$1.5 λ to $\sim$10.0 λ at the operating frequency). This translates to an increase in the number of unknowns from 29 468 to 175 426. The average grid size for all cases is approximately 0.25 λ.

It can be seen that the proposed multilevel preconditioner leads to superior convergence of the iterative solution. The number of iterations varies from eight for the shortest line to 14 for the longest line. This increase with the electrical length of the structure is attributed to the numerical dispersion error, which also increases with the electrical length. The required CPU time increases almost linearly from 30.65 to 326.16 s. For the sake of comparison, the convergence of the iterative solution using the diagonal-preconditioned conjugate gradient (DCG) method is also shown. Clearly, its performance is poor, with the number of iterations increasing linearly with the number of unknowns. More importantly, the required CPU time increases quadratically with the number of unknowns. Other incomplete factorization-based preconditioners exhibit fairly similar performance with the DCG, both in terms of the number of iterations and CPU time.

The next example considers the electromagnetic analysis of the waveguide filter studied in [10]. The geometry and dimensions of the filter are shown in the insert of Fig. 3. The finite-element grid used has an average spatial sampling rate of approximately 7.80 pt/λ at 18 GHz. The number of unknowns at the $H^1(\mathrm{curl})$ level is 42 526. The calculated scattering parameters are in excellent agreement with the results in [10].

The excellent convergence of the proposed preconditioned iterative solver is illustrated in Fig. 4. The required total CPU time

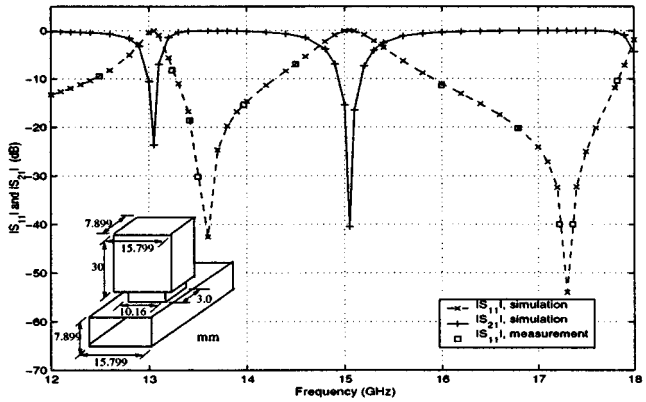

Fig. 3. Magnitude of scattering parameters for the waveguide filter of [10].

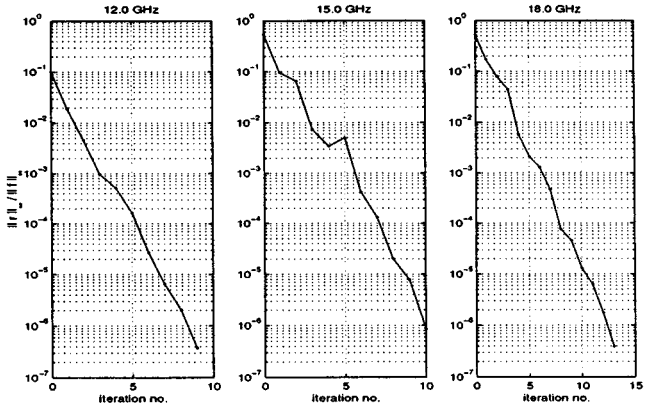

Fig. 4. Convergence behavior of the proposed preconditioner applied to the analysis of the waveguide filter of [10].

TABLE I
CONVERGENCE COMPARISON OF CG SOLVERS AT 15.0 GHz

freq. (GHz)		15.0
No preconditoner	# of iter.	4394
	cpu (sec)	1339.22
Single-level A-V	# of iter.	58
	cpu (sec)	108.01
Multilevel A-V	# of iter.	11
	cpu (sec)	34.23

at 12, 15, and 18 GHz is 32.91, 34.23, and 39.65 s, respectively. The memory usage is 30 MB.

To demonstrate the superiority of the proposed preconditioners, the convergence performance and behavior of three CG solvers, namely, un-preconditioned, single-level, and multilevel potential preconditioned at 15.0 GHz are compared in Table I and Fig. 5(a). The single-level potential preconditioner is obtained by neglecting steps (i.e., 3b–3d) in the multilevel pseudocode. Clearly, its performance is better than the one of the un-preconditioned CG because it renders the search vectors divergence free. Its performance is further improved by the multilevel potential preconditioner because of its effective handling of the physical low-frequency modes. In Fig. 5(b), a comparison of the multilevel potential preconditioned CG and

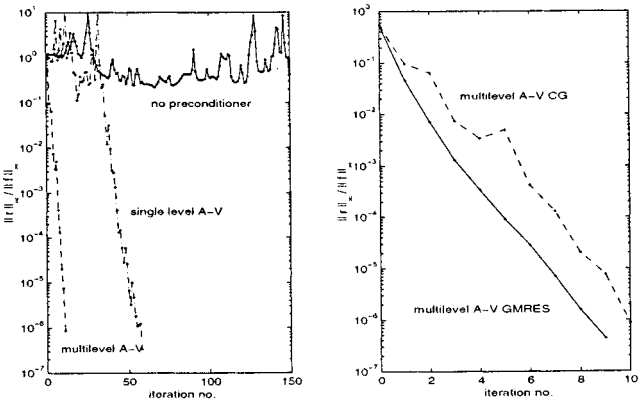

(a) (b)

Fig. 5. (a) Convergence comparison of three CG solvers. (b) Convergence comparison of multilevel preconditioned CG and GMRES.

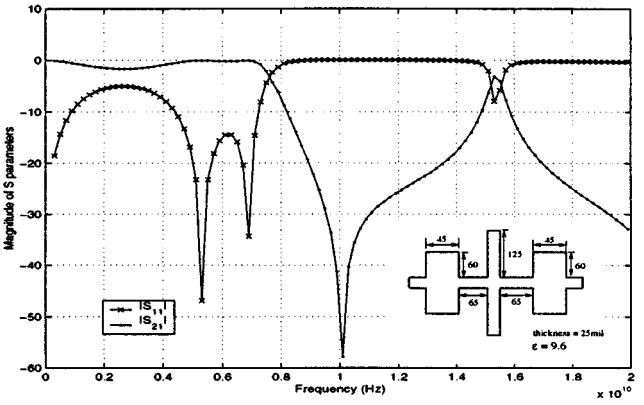

Fig. 6. Magnitude of the scattering parameters of the low-pass filter analyzed in [11].

GMRES at 15.0 GHz is provided to demonstrate the similarity in their convergence behavior.

The last example considers the FEM analysis of the low-pass microstrip filter shown in the insert of Fig. 6. A 345 × 375 × 150 mil^3 computational domain is used with the absorbing boundary set 75 mil above the filter. The finite-element grid used had an average spatial sampling rate of 8.5 pt/λ. The number of unknowns at the $H^1(\mathrm{curl})$ level is 88 708. The calculated scattering parameters are in good agreement with the data in [11]. It is noted that the mesh used is rather uniform. Use of a nonuniform mesh with higher density in the immediate vicinity of the metallization is expected to improve solution accuracy.

Once again, the convergence of the proposed iterative solver is excellent, as demonstrated by the curves in Fig. 7. The required CPU times for the solution at 0.5, 9.0, and 18.0 GHz are 194.54, 209.44, and 219.29 s, respectively. The memory usage is 70 MB.

To test the robustness of the proposed preconditioners, the operating frequency was set to 40.0 GHz. At this frequency, the average grid size is 4.2 pt/λ. The convergence behavior of the three CG solvers, depicted in Fig. 8, clearly demonstrates the robustness of the proposed single-level and multilevel potential preconditioners.

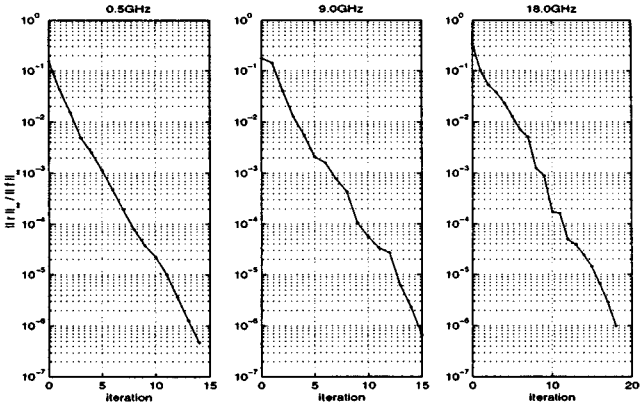

Fig. 7. Convergence behavior of the proposed preconditioner.

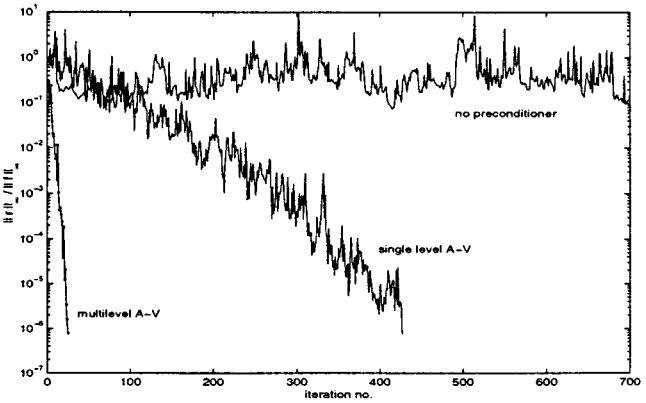

Fig. 8. Convergence comparison of three CG solvers.

VII. Concluding Remarks

In conclusion, an efficient hierarchical multilevel potential preconditioner has been proposed and demonstrated for the robust, expedient and broad-band finite-element analysis of microwave devices. Through the combination of the hierarchical vector and scalar potential formulation with a hierarchical multilevel preconditioning technique, the ill conditioning of the FEM matrix is avoided, and a fast converging iterative FEM solver is obtained. Since the proposed preconditioner requires the direct factorization of the FEM matrix at the $H^0(\mathrm{curl})$ level, its capability to solve very large problems is limited. A way to overcome this limitation is to hybridize it with the nested multigrid potential preconditioner [6]. The merits of this hybridization are currently under investigation.

References

[1] A. C. Polycarpou, P. A. Tirkas, and C. A. Balanis, "The finite-element method for modeling circuits and interconnects for electromagnetic packaging," *IEEE Trans. Microwave Theory Tech.*, vol. 45, pp. 1868–1874, Oct. 1997.

[2] R. Dyczij-Edlinger and O. Biro, "A joint vector and scalar potential formulation for driven high frequency problems using hybrid edge and nodal finite elements," *IEEE Trans. Microwave Theory Tech.*, vol. 44, pp. 15–23, Jan. 1996.

[3] R. Dyczij-Edlinger, G. Peng, and J. F. Lee, "A fast vector-potential method using tangentially continuous vector finite elements," *IEEE Trans. Microwave Theory Tech.*, vol. 46, pp. 863–868, June 1999.

[4] R. Beck and R. Hiptmair, "Multilevel solution of the time-harmonic Maxwell's equations based on edge elements," *Int. J. Numer. Methods Eng.*, vol. 45, pp. 901–920, 1999.

[5] Y. Zhu and A. C. Cangellaris, "Nested multigrid vector and scalar potential finite element method for fast computation of two-dimensional electromagnetic scattering," *IEEE Trans. Antennas Propagat.*, to be published.

[6] Y. Zhu and A. C. Cangellaris, "Robust multigrid preconditioner for fast finite element modeling of microwave devices," *IEEE Microwave Wireless Comp. Lett.*, vol. 11, pp. 416–418, Oct. 2001.

[7] G. Peng, R. Dyczij-Edlinger, and J. F. Lee, "Hierarchical methods for solving matrix equations from TVFEM for microwave components," *IEEE Trans. Magn.*, vol. 35, pp. 1474–1477, May 1999.

[8] G. Peng, "Multigrid preconditioning in solving time-harmonic wave propagation problems using tangential vector finite elements," Ph.D. dissertation, Elect. Comput. Eng. Dept., Worcester Polytech. Inst., Worcester, MA, Nov. 1997.

[9] Y. Zhu and A. C. Cangellaris, "Hierarchical finite element basis function spaces for tetrahedral elements," in *Proc. Appl. Comput. Electromagn. Soc. Meeting*, Monterey, CA, Mar. 2001, pp. 69–74.

[10] T. Sieverding and F. Arndt, "Field theoretic CAD of open or aperture matched T-junction coupled rectangular waveguide structures," *IEEE Trans. Microwave Theory Tech.*, vol. 40, pp. 353–363, Feb. 1992.

[11] J. E. Bracken, D. K. Sun, and Z. Cendes, "S-domain methods for simultaneous time and frequency characterization of electromagnetic devices," *IEEE Trans. Microwave Theory Tech.*, vol. 47, pp. 1277–1290, Sept. 1998.

Yu Zhu (S'00) received the B.S. degree from Nanjing University, Nanjing, China, in 1995, the M.S. degree from The Ohio State University, Columbus, in 1998, both in electrical engineering, and is currently working toward the Ph.D. degree in electrical and computer engineering at the University of Illinois at Urbana-Champaign (UIUC).

From 1997 to 1998, he was a Graduate Research Assistant with the Electro-Science Laboratory, The Ohio State University. Since 1999, he has been a Graduate Research Assistant with Center for Computational Electromagnetics, UIUC. His research interests include computational electromagnetics, FEMs, integral-equation techniques, and microwave engineering.

Mr. Zhu was the recipient of the 2001 Y. T. Lo Outstanding Graduate Research Award presented by the Department of Electrical and Computer Engineering, UIUC.

Andreas C. Cangellaris (M'86–SM'96–F'00) received the M.S. and Ph.D. degrees in electrical and computer engineering from the University of California at Berkeley, in 1983 and 1985, respectively.

He is currently a Professor of electrical and computer engineering with the University of Illinois at Urbana Champaign (UIUC). Prior to joining UIUC, he was on the faculty of the Electrical and Computer Engineering, University of Arizona, initially as an Assistant Professor (1987–1992) and then as an Associate Professor (1992–1997). Prior to that, he was a Senior Research Engineer with the Electronics Department, General Motors research Laboratories, Warren, MI (1985–1987). His research has concerned the area of applied and computational electromagnetics with emphasis on their application to electrical modeling and simulation of RF/microwave components and systems, high-speed digital interconnects at the board, package, and chip level, as well as the modeling and simulation of electromagnetic compatibility and electromagnetic interference. He has co-authored over 150 refereed papers and three book chapters on topics related to computational electromagnetics and interconnects and package modeling and simulation. Over the past 14 years, he has supervised the development of electromagnetic modeling methodologies and numerous computer modeling and simulation tools for high-speed/high-frequency signal integrity-driven applications, which have been transferred successfully to industry.

Prof. Cangellaris is an active member of the IEEE Microwave Theory and Techniques Society (IEEE MTT-S), the IEEE Components Packaging and Manufacturing Technology Society, the IEEE Antennas and Propagation Society (IEEE AP-S), and the IEEE Magnetics Society. He serves as member of Technical Program Committees for major conferences and symposia sponsored by these societies. He has served as associate editor for the IEEE Transactions on Antennas and Propagation and is currently associate editor for the IEEE Transactions on Advanced Packaging and the IEEE Press Series on Electromagnetic Fields and Waves. He is the co-founder of the IEEE Topical Meeting on Electrical Performance of Electronic Packaging.